

# Calculation of the ambient dose equivalent $H^*(10)$ from gamma-ray spectra obtained with scintillation detectors



Ramon Casanovas\*, Elena Prieto, Marçal Salvadó

Unitat de Física Mèdica, Facultat de Medicina i Ciències de la Salut, Universitat Rovira i Virgili, Reus, Tarragona, ES-43201 Spain

## ARTICLE INFO

### Keywords:

$H^*(10)$   
Scintillation gamma-ray spectrometry  
 $\text{LaBr}_3(\text{Ce})$   
Monte Carlo simulation

## ABSTRACT

The measurement of the ambient dose equivalent  $H^*(10)$  with automatic real-time radioactivity monitors using gamma-ray spectrometry provides valuable information at short integration times and serves as an alternative to conventional peak analysis of spectra. In this paper, a full methodology for the calculation of this quantity using Monte Carlo (MC) simulations is described and applied to real spectrometric measurements with  $\text{LaBr}_3(\text{Ce})$  scintillation detectors. The methodology involves the calculation of the fluence-to- $H^*(10)$  conversion factors and a method for obtaining the fluence from gamma-ray spectra. The combination of these two elements makes it possible to calculate the  $H^*(10)$ . The obtained results are compared with the  $H^*(10)$  measurements of a Geiger-Müller (GM) detector. Finally, the necessary activity concentration to produce a certain increment on the  $H^*(10)$  is discussed for some isotopes. This is used to discuss the analysis capabilities of the spectrometric detectors when compared to GM ones.

## 1. Introduction

Article 35 of the Euratom Treaty (2000/473/Euratom, 2000) requires each Member State to establish the necessary facilities to carry out real-time monitoring of the level of radioactivity in air, water, and soil and to ensure compliance with the basic standards. Following these requirements, there is an automatic real-time surveillance network in Catalonia (ES-E, Spain-East).

Recently, a project for the implementation of environmental radioactivity monitors using real-time gamma-ray spectrometry in this network has started. The project began after the findings of a previous study (Casanovas et al., 2011), which recommended this implementation for obtaining new and better radiological information.

Therefore, three different types of radiation monitors using either NaI(Tl) or  $\text{LaBr}_3(\text{Ce})$  scintillation detectors have been recently developed, calibrated, and implemented into the Catalan real-time surveillance network: a water monitor (Casanovas et al., 2013), an aerosol monitor using a particulate filter (RARM-F) (Casanovas et al., 2014a), and a monitor using two shielded detectors measuring directly to the environment (RARM-D2) (Casanovas et al., 2014b).

However, to obtain real-time information from gamma-ray spectrometry (i.e. to obtain information in short integration times, e.g. 10 min), conventional peak analysis of gamma-ray spectra may not be useful as a consequence of having poor statistics. For this, other analysis methods are being developed to maximize the information extracted from the spectra. In particular, one of them is obtaining the

ambient dose equivalent  $H^*(10)$  from gamma-ray spectra.

The ambient dose equivalent  $H^*(10)$  is recommended by the ICRP as the operational quantity for assessing effective dose in area monitoring (ICRP 103, 2007). In most practical situations of external radiation exposure, the ambient dose equivalent fulfils the aim of providing a conservative estimate or upper limit for the value of the limiting quantities.

The calculation of dosimetric quantities from gamma-ray or neutron spectra has been addressed in other studies by using different methodologies applied to several types of detectors (Camp and Vargas, 2014; Kim et al., 2002; Sato et al., 2005; Terada et al., 1980).

In this work, a full methodology for the calculation of the ambient dose equivalent  $H^*(10)$  using Monte Carlo (MC) simulations is described and applied to real spectrometric measurements with  $\text{LaBr}_3(\text{Ce})$  scintillation detectors.

## 2. Materials

### 2.1. Detectors

The gamma-ray spectrometry detectors that were used in this study were two 2"x2"  $\text{LaBr}_3(\text{Ce})$  scintillation detectors, which are part of the RARM-D2 monitor (Casanovas et al., 2014b). RARM-D2 monitor consists of two scintillation detectors (see Fig. 1), one pointing up (1) and the other pointing down (2), which are shielded with Pb (3) to permit the separate measurement of the airborne isotopes with respect

\* Corresponding author.

E-mail address: [ramon.casanovas@urv.cat](mailto:ramon.casanovas@urv.cat) (R. Casanovas).

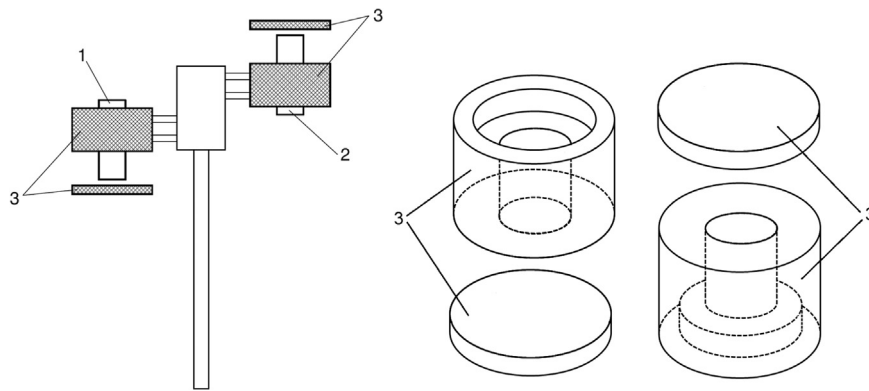


**Fig. 1.** General scheme of the RARM-D2 (left) and detailed scheme of the Pb shielding (right). The main elements are: detector pointing up (1), detector pointing down (2) and Pb shielding (3).

to the deposited isotopes. Both  $\text{LaBr}_3(\text{Ce})$  detectors were BrillanCe™380 from Saint-Gobain Crystals. Each of the detectors was connected to a multichannel pulse-height analyzer of 2000 channels.

For comparison purposes, a Geiger-Müller (GM) Intelligent Gamma Probe IGS421 from EnviroNet was also used (EnviroNet, 2011). This GM monitor is composed of three detectors (two for low dose rates and one for higher ones) that are calibrated to measure the ambient dose equivalent rate in the range from 10 nSv/h to 10 Sv/h.

Both monitors, the RARM-D2 and the GM, were installed in the owner controlled area of the Ascó Nuclear Power Plant, in an open environment far from buildings or vegetation to avoid interferences with measurements. To ensure that detectors were exposed to the same radiation field, the monitors were positioned so that their active parts were at the same height (at about 2 m).

## 2.2. Radioactive sources

The certified radioactive sources that were used in this study for calibration purposes were five point sources of  $^{241}\text{Am}$ ,  $^{133}\text{Ba}$ ,  $^{137}\text{Cs}$ ,  $^{60}\text{Co}$ , and  $^{152}\text{Eu}$ . Besides, an  $^{238}\text{U}$  ore was used to calibrate through some of the gamma lines of its progeny ( $^{226}\text{Ra}$ ,  $^{214}\text{Bi}$ ,  $^{214}\text{Pb}$ , etc.).

## 3. $H^*(10)$ calculation method

For the measurement of the ambient dose equivalent  $H^*(10)$  with scintillation detectors using gamma-ray spectrometry, two elements are necessary: the conversion factors from gamma-ray fluence to  $H^*(10)$  and the calculation of gamma-ray fluence from spectra. Combining these two elements, it is possible to obtain the  $H^*(10)$  from spectra.

### 3.1. Calculation of the fluence-to- $H^*(10)$ conversion factors

#### 3.1.1. $H^*(10)$ and ICRU sphere definition

The definition provided by the International Commission on Radiation Protection (ICRP 103, 2007) for the  $H^*(10)$  is: “The ambient dose equivalent,  $H^*(10)$ , at a point in a radiation field, is the dose equivalent that would be produced by the corresponding expanded and aligned field in the ICRU sphere at a depth of 10 mm on the radius vector opposing the direction of the aligned field”. The ICRU sphere (ICRU 39, 1985) is a 30 cm diameter sphere of unit density (1 g/cm<sup>3</sup>) tissue-equivalent material (mass composition: 76.2% O, 11.1% C, 10.1% H and 2.6% N).

#### 3.1.2. Monte Carlo simulations

The conversion factors  $F$  from gamma-ray fluence  $\Phi$  to ambient

dose equivalent  $H^*(10)$  were calculated using Monte Carlo simulations with the EGS5 code system (Hirayama et al., 2005), which is a general-purpose package that enables the simulation of the coupled transport of electrons and photons in an arbitrary geometry. For this, an EGS5 user code was specifically programmed, which controls the EGS5 subroutines and contains all of the information about the radiation source (type of particles, energy of the particles and geometrical distribution) and the details of the ICRU sphere (geometry, density and composition).

Thus, several beams of  $10^7$  monoenergetic gamma rays covering the range from 0 to 2000 keV were simulated. The gamma rays were distributed in a 30 cm diameter circle and emitted towards the ICRU sphere following parallel trajectories and propagated through the vacuum. For each of the gamma-ray energies, the absorbed dose in a 1 mm-side cube was recorded. The cube was located at a depth of 10 mm in the sphere, according to the  $H^*(10)$  definition. Then, at those energies, the conversion factors  $F$  were calculated by dividing the simulated fluence with the absorbed dose in the cube at a depth of 10 mm.

To improve statistics without the need of increasing the number of simulated gamma rays, a variance reduction technique was used. This technique consists in increasing the number of gamma rays that deposit energy in the small cube where the dose is computed. As the cube is located around the axis, this can be achieved using a distribution of gamma rays that is more peaked on the axis. Thus, the distribution given by Eq. (1) was used (Ferrari and Pelliccioni, 1994):

$$r = R \cdot \xi^{\frac{1}{1-\alpha}} \quad (1)$$

where  $r$  is the radial coordinate,  $R$  the radius of the gamma rays beam,  $\xi \in U(0,1)$  a random number, and  $\alpha = 1/2$  a constant parameter.

To obtain an unbiased result, the scored quantities need to be weighted with the statistical weight  $w$  given in Eq. (2):

$$w = \frac{2}{1-\alpha} \frac{r^{1+\alpha}}{R^{1+\alpha}} \quad (2)$$

Statistical uncertainties were estimated by performing all calculations in several batches and computing the standard deviation of the average (Casanovas et al., 2012a).

### 3.2. Calculation of the gamma-ray fluence from spectra

When a gamma ray interacts with a scintillation detector, it can either deposit all of its energy or suffer a partial absorption (e.g. a Compton interaction after which the resulting electron deposits its energy in the detector and the gamma ray leaves the detector). Thus, the response of a scintillation detector does not only include full energy peaks corresponding to the energies of the gamma-rays emitted by the source, but also the effect of several partial absorptions.

The relation between the measured spectrum  $\vec{M}$  and the fluence of incident gamma-ray spectrum  $\vec{\phi}$  can be written as a matrix equation:

$$M = R \cdot \phi \quad \begin{pmatrix} M_1 \\ M_2 \\ \vdots \\ M_n \end{pmatrix} = \begin{pmatrix} R_{11} & R_{12} & \cdots & R_{1n} \\ R_{21} & \ddots & & R_{2n} \\ \vdots & & \ddots & \vdots \\ R_{n1} & R_{n2} & \cdots & R_{nn} \end{pmatrix} \begin{pmatrix} \phi_1 \\ \phi_2 \\ \vdots \\ \phi_n \end{pmatrix} \quad (3)$$

where  $\vec{M}$  and  $\vec{\phi}$  are  $n \times 1$  vectors representing the measured spectrum and the incident gamma-ray fluence spectrum, respectively, and  $R$  an  $n \times n$  matrix containing the information of the detector response (including the effect of the partial absorptions). A square response matrix was specifically chosen to ease solving the system of linear equations.

The response matrix  $R$  was calculated by means of Monte Carlo simulations using EGS5. For this, a user code was programmed to include all the information about the source term and the detector geometry, and to record the necessary quantities. For the calculations, the dimension of vectors and matrices was set to  $n=40$ , which was identified as appropriate in another study (Camp and Vargas, 2014). The  $R$  matrix was built by recording the response of the detector to different gamma ray energies, ranging from 0 to 2000 keV in steps of 50 keV (40×40 matrix). The gamma rays were distributed in a circle of 15 cm radius, similarly to the ICRU sphere calculations.

### 3.3. Calculation of $H^*(10)$

After having the fluence-to- $H^*(10)$  conversion factors and the response matrix, the calculation of the  $H^*(10)$  from gamma-ray spectra is straightforward. If  $\vec{F}$  is a  $n \times 1$  vector containing the conversion factors from fluence to  $H^*(10)$  at the same energies than the components of  $\vec{M}$  and  $\vec{\phi}$ , then the  $H^*(10)$  can be written as the following scalar product:

$$H^*(10) = F \cdot \phi \quad H^*(10) = \begin{pmatrix} F_1 & F_2 & \cdots & F_n \end{pmatrix} \cdot \begin{pmatrix} \phi_1 \\ \phi_2 \\ \vdots \\ \phi_n \end{pmatrix} \quad (4)$$

From Eq. (3), the fluence vector can be written as:

$$\vec{\phi} = R^{-1} \cdot \vec{M} \quad (5)$$

And combining Eq. (4) and Eq. (5):

$$H^*(10) = F \cdot \phi = F \cdot R^{-1} \cdot M = \chi \cdot M \quad H^*(10) = \begin{pmatrix} \chi_1 & \chi_2 & \cdots & \chi_n \end{pmatrix} \cdot \begin{pmatrix} M_1 \\ M_2 \\ \vdots \\ M_n \end{pmatrix} = \chi_1 M_1 + \chi_2 M_2 + \cdots + \chi_n M_n \quad (6)$$

where the vector  $\chi$  is defined as:

$$\chi \equiv F \cdot R^{-1} \begin{pmatrix} \chi_1 & \chi_2 & \cdots & \chi_n \end{pmatrix} \equiv \begin{pmatrix} F_1 & F_2 & \cdots & F_n \end{pmatrix} \cdot \begin{pmatrix} R_{11} & R_{12} & \cdots & R_{1n} \\ R_{21} & \ddots & & R_{2n} \\ \vdots & & \ddots & \vdots \\ R_{n1} & R_{n2} & \cdots & R_{nn} \end{pmatrix}^{-1} \quad (7)$$

From Eq. (6), the ambient dose equivalent  $H^*(10)$  can be calculated by dividing the measured spectra in  $n$  Regions of Interest (ROIs), adding the counts in each of the ROIs ( $M_i$ ), and summing them weighted by the calculated  $\chi_i$  factors.

However, as a consequence of the smooth variation of the  $\chi_i$  factors, it is possible to expand the calculations to all channels in the spectrum, avoiding the need of adding the counts in each of the ROIs and obtaining more precision in the calculations. Thus, the  $\chi_i$  factors are fitted to a sixth order polynomial to get the  $\bar{\chi}_j$  factors for each of the

channels. Then, the calculation of  $H^*(10)$  is performed using:

$$H^*(10) = \sum_{j=1}^{N_{channels}} \bar{\chi}_j \cdot C_j \quad (8)$$

where  $C_j$  are the counts in the channel  $j$ .

### 3.4. Experimental spectra preparation

Before using Eq. (8) for  $H^*(10)$  calculation, some steps need to be performed to prepare the acquired spectra. These steps encompass spectra stabilization, energy calibration, and background subtraction.

#### 3.4.1. Spectra stabilization

When detectors are operated under unstable temperature conditions in the environment, a peak shift in spectra and a consequent spectral distortion is observed. Thus, it is necessary to stabilize the acquired spectra.

For this purpose, software was specifically designed and used to perform the stabilization of spectra. This software automatically searches the position of reference peaks and uses them to stabilize the spectrum by applying a method that was previously developed in another study (Casanovas et al., 2012b).

#### 3.4.2. Energy calibration

After spectrum stabilization, the energy calibration was applied using a 2nd grade polynomial. In a previous study (Casanovas et al., 2012a), this function was identified as appropriate for describing the relation between energy and channel number. This relation was established experimentally using the radioactive sources described in Section 2.2.

#### 3.4.3. Background subtraction

Finally, before using Eq. (8), the self-contamination background of the LaBr<sub>3</sub>(Ce) detector spectra (Quarati et al., 2012) needed to be removed. For doing so, a reference spectrum was recorded in a low background environment and was subtracted to all the spectra before the calculation of the  $H^*(10)$ .

### 3.5. $H^*(10)$ vs concentration of activity

After having a method for the calculation of  $H^*(10)$  from spectra, it is possible to determine the activity concentration (Bq/m<sup>3</sup>) of a certain isotope that is necessary to produce a certain  $H^*(10)$  increment.

For doing so, it is necessary to recall to the detector efficiency curve, which provides the relation between the counts per second (cps) in the detector and the activity concentration (Bq/m<sup>3</sup>) at different gamma-ray energies. This curve was calculated in a previous study using Monte Carlo simulations (Casanovas et al., 2014b).

Having the relation between the cps and Bq/m<sup>3</sup> and the methodology for calculating the  $H^*(10)$  from the spectra (cps for different gamma-ray energies), it is possible to establish a relationship between the activity concentration and the  $H^*(10)$ .

In this study, the interest was focused on calculating the activity concentration of some isotopes that produce an  $H^*(10)$  increment equivalent to the Investigation Level that was defined in a previous study for GM monitors (Casanovas et al., 2011), which corresponds to an increment of 0.008  $\mu$ Sv/h. The calculations were performed for the following isotopes: <sup>241</sup>Am, <sup>131</sup>I, <sup>137</sup>Cs and <sup>60</sup>Co. These isotopes are of interest in environmental gamma-ray spectrometry and cover a broad range of gamma-ray energies.

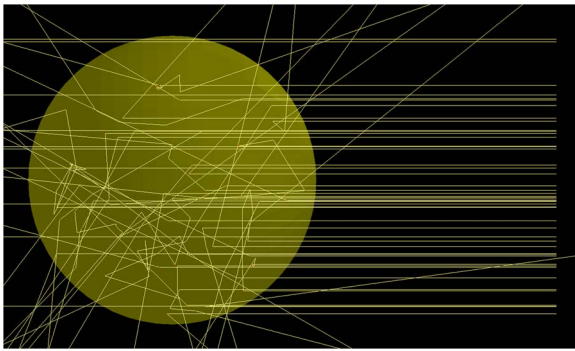


Fig. 2. MC simulation of a parallel beam of gamma-rays distributed in a circle of 15 cm radius and incident to the ICRU sphere where several interactions take place.

## 4. Results and discussion

### 4.1. Fluence-to- $H^*(10)$ conversion factors

The geometrical arrangement for the MC simulations is shown in Fig. 2, which includes a parallel beam of gamma rays distributed in a circle of 15 cm radius and incident to the ICRU sphere where several interactions take place.

The calculated fluence-to- $H^*(10)$  conversion factors are shown in Fig. 3. The obtained values were compared with those from ICRP 74 publication (ICRP 74, 1996) and found to be in good agreement with them.

### 4.2. Calculation of the gamma-ray fluence from spectra

For the calculation of the response matrix  $R$ , the arrangement shown in Fig. 4 was used, which included the detector (geometry and materials composition) and the parallel beam of gamma rays.

The obtained results for the response matrix  $R$  were combined with the fluence-to- $H^*(10)$  conversion factors to calculate the  $\chi_i$  factors using Eq. (7). The calculated  $\chi_i$  factors from cps to nSv/h are shown in Fig. 5.

### 4.3. Calculation of $H^*(10)$

The calculation of  $H^*(10)$  was performed separately at each of the two detectors of the RARM-D2 monitor by using Eq. (8) with the interpolated coefficients from Fig. 5. Then, both values were added to obtain the total  $H^*(10)$ . This enabled the comparison with the GM monitor, which is sensible to both gamma radiation coming from the airborne isotopes and from the soil isotopes.

#### 4.3.1. $H^*(10)$ comparison

By way of example, a comparison between the ambient dose equivalent rate  $H^*(10)$  obtained during one month from the  $\text{LaBr}_3(\text{Ce})$  spectrometric detectors and the measurements from the GM monitor is provided in Fig. 6.

The results in Fig. 6 show that both monitors provide similar relative measurements. The observed  $H^*(10)$  fluctuations are consequence of daily variations of  $^{222}\text{Rn}$  and  $^{220}\text{Rn}$  concentrations in air, which strongly depend on different meteorological variables (insolation, atmospheric pressure, humidity, rain, etc.). Radon isotopes emanate from the subsoil to the atmosphere and decay to different daughters that are gamma emitters (such as  $^{214}\text{Bi}$ ,  $^{214}\text{Pb}$  or  $^{208}\text{Tl}$ ). As it can be observed between day 21 and day 25, this effect becomes relevant during rain episodes.

Regarding absolute values, the results in Fig. 6 show that the GM monitor provides higher values than that calculated for the  $\text{LaBr}_3(\text{Ce})$  detector. On average, the absolute differences between them were

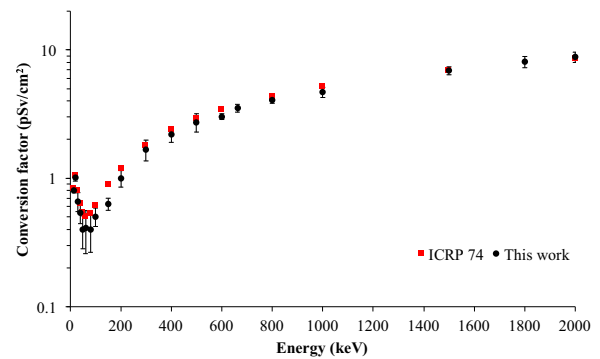


Fig. 3. Fluence-to- $H^*(10)$  conversion factors calculated in this study (circles) and compared with those in ICRP 74 publication (squares).

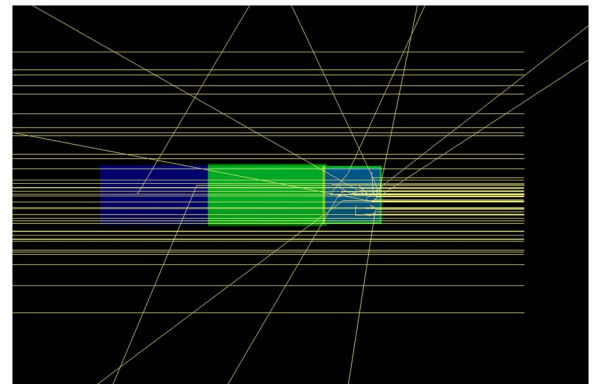


Fig. 4. MC simulation of a parallel gamma rays beam distributed in a 15 cm radius circle and incident to a scintillation detector.

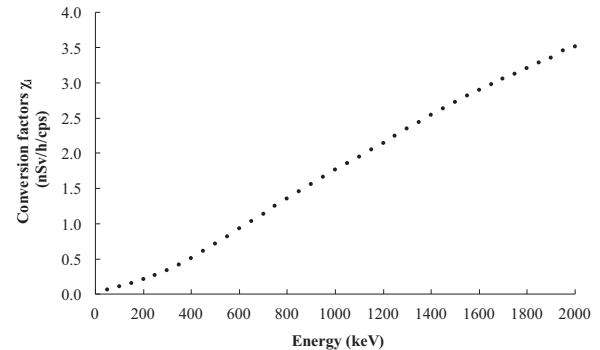


Fig. 5. Conversion factors  $\chi_i$  (from cps to nSv/h) for  $H^*(10)$  calculation.

about 0.02  $\mu\text{Sv/h}$ . However, the radiological increments above the average value were of similar magnitude.

Based on the information that is given in the technical data sheet of the GM monitor (Envinet, 2011), an overestimation of the dose rate in the GM monitor was expected since it provides a higher response for gamma rays with energies above that of  $^{137}\text{Cs}$  (as some from  $^{226}\text{Ra}$  progeny that are always present in the environment). An overestimation of +67% is expected for 2.5 MeV gamma rays.

Similar results on  $H^*(10)$  overestimation with GM monitors were also observed in another study (Sáez-Vergara et al., 2002), where different GM monitors were compared with the readings of an ion chamber and some TLDs. The same study concluded that the GM detectors have an inherent background that needs to be compensated and that they usually provide a higher response to gamma rays with energies above 662 keV as a consequence of being only calibrated with  $^{137}\text{Cs}$ .

Another justification of the GM providing greater values is that the cosmic radiation component is difficult to be measured separately from



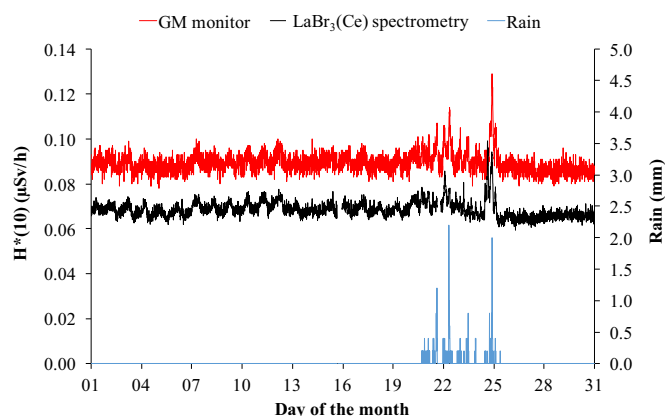


**Fig. 6.** Comparison of the ambient dose equivalent rate  $H^*(10)$  obtained with a LaBr<sub>3</sub>(Ce) spectrometry detector (black) and obtained with a GM monitor (red). The rainfall during the period is also provided (blue). (For interpretation of the references to color in this figure legend, the reader is referred to the web version of this article.)

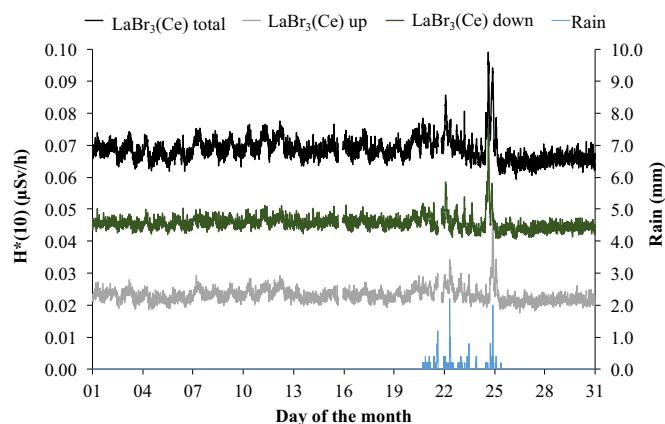


**Fig. 7.** Contribution to the total  $H^*(10)$  (black) of the up detector (gray) and down detector (green) of RARM-D2. The rainfall during the period is also provided (blue). (For interpretation of the references to color in this figure legend, the reader is referred to the web version of this article.)

**Table 1**

Activity concentration increments for different isotopes to produce an  $H^*(10)$  increment of 0.008  $\mu\text{Sv/h}$  in a 2"x2" LaBr<sub>3</sub>(Ce) detector.

Isotope	Activity concentration (Bq/m <sup>3</sup> )
<sup>241</sup> Am	48.6
<sup>131</sup> I	19.1
<sup>137</sup> Cs	51.1
<sup>60</sup> Co	141.4

the internal background of the LaBr<sub>3</sub>(Ce) detectors, and thus, it is lost when subtracting this internal background. Consequently, this component must be obtained by other means and added to the measurements. A value of 0.033  $\mu\text{Sv/h}$  for the cosmic dose rate in Barcelona is given in (Camp and Vargas, 2014), which could be assumed as similar to that in the location where the experimental measurements of this study were carried out.

Finally, it is important to remark that if the internal background of the LaBr<sub>3</sub>(Ce) had not been subtracted, and so the counts had been interpreted as external dose rate, it would have added a surplus to the ambient dose equivalent rate  $H^*(10)$  of 0.115  $\mu\text{Sv/h}$  (more than 1 mSv/y). The background subtraction process could also be a source of uncertainty that justifies the differences with the GM.

In view of the discrepancies on the obtained results, a more complete study of inter-comparison needs to be performed. The inter-comparison should be done by using other type of detectors (e.

g. TDLs or proportional counters) that could provide other estimates of the  $H^*(10)$ .

#### 4.3.2. $H^*(10)$ contributions

The contribution to the  $H^*(10)$  of the upwards- and downwards-pointing detectors of the RARM-D2 is not the same (see Fig. 7). In average, the contribution of the up detector is about 1/3 and the one for the down detector is about 2/3. This is a consequence of the vertical distribution of the radon concentration, which is higher close to the ground and becomes lower with height as a consequence of its atmospheric dispersion.

#### 4.4. $H^*(10)$ vs concentration of activity

The results for the activity concentration of some isotopes that produce an  $H^*(10)$  increment of 0.008  $\mu\text{Sv/h}$  in a LaBr<sub>3</sub>(Ce) detector are provided in Table 1. The calculated activity concentrations provide an idea of the contribution to the  $H^*(10)$  of each of the isotopes, considering that they emit gamma rays at different energies and with different probabilities.

The same methodology could be applied in the other way to obtain the  $H^*(10)$  increment that is produced after a given concentration of activity. This could be valuable in assessing doses and establishing radiation protection measures.

Results in Table 1 can be also interpreted as the necessary activity concentration to produce the  $H^*(10)$  increment in the GM monitor, and so they can be also used to compare the sensitivity of both types of detectors to gamma rays.

By way of example, the necessary activity concentration of <sup>137</sup>Cs for triggering the investigation level in the GM monitors, which is set at 0.008  $\mu\text{Sv/h}$ , is 51.1 Bq/m<sup>3</sup>. However, the Minimum Detectable Activity Concentration (MDAC) in a 10 min spectrum for <sup>137</sup>Cs is 5.3 Bq/m<sup>3</sup> (Casanovas et al., 2014b). Hence, it can be concluded that the spectrometric capabilities would provide better sensitivity, since the presence of <sup>137</sup>Cs would be detected before using conventional spectrometric analysis rather than realizing an abnormal increment of the ambient dose equivalent  $H^*(10)$ .

## 5. Conclusions

A full methodology for the calculation of the ambient dose equivalent  $H^*(10)$  in automatic real-time radioactivity monitors using gamma-ray spectrometry was provided. This methodology encompasses the calculation of the fluence-to- $H^*(10)$  conversion factors and a method for obtaining the fluence from gamma-ray spectra. Both calculations were performed using Monte Carlo simulations with the EGS5 code system.

The methodology was applied in a LaBr<sub>3</sub>(Ce) detector and the obtained results for the  $H^*(10)$  were compared with the measurements of a GM detector. In view of the results, a more complete study of inter-comparison needs to be performed.

The method was also used for calculating the necessary activity concentrations of some isotopes to produce a determined increment on the  $H^*(10)$ . This was used to compare the capabilities of gamma-ray spectrometry with that of the GM detector.

Finally, the developed methodology can be adapted for obtaining the  $H^*(10)$  in other types of spectrometric detectors, either detectors with different materials or from different sizes, and the calculations can be also performed for other gamma-ray energy ranges.

## Acknowledgments

The work was partially financed by the Consejo de Seguridad Nuclear (CSN, Nuclear Safety Council) of Spain [funding for R & D projects related to radiation protection, BOE No. 178 of 26<sup>th</sup> July 2012]

and the *Servei de Coordinació d'Activitats Radioactives* (SCAR, Radioactive Activities Coordination Service) of the Generalitat de Catalunya [administrative contract for research and data analysis associated with the monitors of the environmental radioactivity surveillance network of the Generalitat de Catalunya, EMO 2013 613, Lot 2]. The Monte Carlo simulations were performed in the supercomputers of the *Consorci de Serveis Universitaris de Catalunya* (CSUC).

## References

- 2000/473/Euratom, 27 July 2000. Commission Recommendation of 8 June 2000, Official Journal of the European Commission, No. 191. (Available from: [http://ec.europa.eu/energy/nuclear/radioprotection/doc/legislation/00473\\_en.pdf](http://ec.europa.eu/energy/nuclear/radioprotection/doc/legislation/00473_en.pdf))
- Camp, A., Vargas, A., 2014. Ambient dose estimation  $H^*(10)$  from  $\text{LaBr}_3(\text{Ce})$  Spectra. *Radiat. Prot. Dosim.* 160, 264–268.
- Casanovas, R., Morant, J.J., Lopez, M., Hernandez-Giron, I., Batalla, E., Salvadó, M., 2011. Performance of data acceptance criteria over 50 months from an automatic real-time environmental radiation surveillance network. *J. Environ. Radioact.* 102, 742–748.
- Casanovas, R., Morant, J.J., Salvadó, M., 2012a. Energy and resolution calibration of NaI (Tl) and  $\text{LaBr}_3(\text{Ce})$  scintillators and validation of an EGS5 Monte Carlo user code for efficiency calculations. *Nucl. Instrum. Methods Phys. Res. A* 675, 78–83.
- Casanovas, R., Morant, J.J., Salvadó, M., 2012b. Temperature peak-shift correction methods for NaI(Tl) and  $\text{LaBr}_3(\text{Ce})$  gamma-ray spectrum stabilisation. *Radiat. Meas.* 47, 588–595.
- Casanovas, R., Morant, J.J., Salvadó, M., 2013. Implementation of gamma-ray spectrometry in two real-time water monitors using NaI(Tl) scintillation detectors. *Appl. Radiat. Isot.* 80, 49–55.
- Casanovas, R., Morant, J.J., Salvadó, M., 2014a. Development and calibration of a real-time airborne radioactivity monitor using gamma-ray spectrometry on a particulate filter. *IEEE Trans. Nucl. Sci.* 61, 727–731.
- Casanovas, R., Morant, J.J., Salvadó, M., 2014b. Development and calibration of a real-time airborne radioactivity monitor using direct gamma-ray spectrometry with two scintillation detectors. *Appl. Radiat. Isot.* 89, 103–108.
- Envinet. Intelligent Gamma Probe IGS421A/B-H. Technical Data Sheet IGS421A/B-H/00EN/09/2011. (Available at): (<http://www.envinet.com>)
- Ferrari, A., Pelliccioni, M., 1994. On the conversion coefficients from fluence to ambient dose equivalent. *Radiat. Prot. Dosim.* 51, 251–255.
- Hirayama, H., Namito, Y., Bielajew, A.F., Wilderman, S.J., Nelson, W.R., 2005. The EGS5 Code System. SLAC-R-730 and KEK Report 2005–8.
- International Commission on Radiation Units and Measurements, 1985. Determination of Dose Equivalents Resulting from External Radiation Sources. ICRU Report 39.
- International Commission on Radiological Protection, 1996. Conversion Coefficients for Use in Radiological Protection against External Radiation. ICRP Publication 74.
- International Commission on Radiological Protection, 2007. The 2007 Recommendations of the International Commission on Radiological Protection. ICRP Publication 103.
- Kim, E., Endo, A., Yamaguchi, Y., Nakamura, T., Shiomi, T., 2002. Measurement of neutron dose with an organic liquid scintillator coupled with a spectrum weight function. *Radiat. Prot. Dosim.* 102, 31–40.
- Quarati, F.G.A., Khodyuk, I.V., van Eijk, C.W.E., Quarati, P., Dorenbos, P., 2012. Study of  $^{138}\text{La}$  radioactive decays using  $\text{LaBr}_3$  scintillators. *Nucl. Instrum. Methods Phys. Res. A* 683, 46–52.
- Sáez-Vergara, J.C., Romero, A.M., Vila Peña, M., Rodríguez, R., Muñiz, J.L., 2002. The use of passive environmental TLDs in the operation of the Spanish early warning network “REVIRA”. *Radiat. Prot. Dosim.* 101, 249–252.
- Sato, T., Satoh, D., Endo, A., Yamaguchi, Y., 2005. Development of dose monitoring system applicable to various radiations with wide energy ranges. *J. Nucl. Sci. Technol.* 42, 768–778.
- Terada, H., Sakai, E., Katagiri, M., 1980. Environmental gamma-ray exposure rates measured by in-situ  $\text{Ge}(\text{Li})$  spectrometer. *J. Nucl. Sci. Technol.* 17, 281–290.